Proceedings of the 2003 IEEE International Frequency Control Symposium and PDA Exhibition
Jointly with the 17th European Frequency and Time Forum

3-D FEM Eigenvalue Analysis of Relative Impedance and Energy Trapping of Resonant Modes in AT-cut Resonators

Masako Tanaka & Tsutomu Imai, Seiko Epson Corporation, Suwa-city, Nagano, JAPAN
Yook-Kong Yong, Rutgers University, Piscataway, NJ, USA

ABSTRACT

There is currently a need to miniaturize AT-cut resonators. However, the size reduction sometimes sacrifices the resonator's Q-values and crystal impedances. Hence, there is a requirement to develop new resonator designs by changing the cut angles or electrode configurations. For these purposes, the 3-D finite element method is employed as a promising design/analysis and prototyping tool for new quartz resonators. There are generally two types of analyses: Eigenvalue analysis and forced vibration analysis. The eigenvalue analysis of resonant modes in AT-cut resonators has been shown to be accurate in predicting the resonant frequencies as a function of the resonator and electrode geometry. [1,2,3] The forced vibration (steady state) analysis is used to calculate the motional impedance and capacitance in the resonator. In this paper we propose using the eigenvalue analysis for comparing the impedance and energy trapping of the fundamental thickness shear mode of an AT-cut resonator as a function of the resonator and electrode geometries. By comparing and calibrating the numerical results with experimental data, the eigenvalue analysis can efficiently estimate Q-values, crystal impedances, strength of activity dips and frequency- temperature stabilities. The eigenvalue analysis could further generate information useful for choosing resonator and electrode geometry that have higher dimensional tolerance in a fabrication process. The proposed method could be employed to develop a new resonator with a different cut angle and with different electrode configurations. The forced vibration analysis is more cumbersome for these types of analyses.

I. INTRODUCTION

The AT-cut crystal resonators are essential devices in the telecommunication market due to their frequency stability in a wide range of temperatures. The application for the wireless network requires higher frequency stability than the usual property of conventional AT-cut resonators. Many research works to improve their frequency stability were performed to find out new resonators with new cut angles or with new structures in place of using compensation circuit. However designing new resonators has many unpredictable phenomena such as high crystal impedance and coupling with other spurious mode or a different frequency temperature curve. For these purposes, a precise analytical tool for analyzing various resonator structures, which can perform precise eigenvalue analysis in wide range of temperatures, and which can estimate their impedance, will save a lot of time in our experimental studies.

In this paper, we employ 3-D FEM models as our analytical tool. The general assumption on 3-D FEM are that they will need more calculation time and larger memory size than 2-D plate FEM models. However, we model the quartz plate with a single layer of 216-node isoparametric elements with quintic Lagrangian polynomial shape functions, and we have found the model to be more accurate, have smaller number of elements/equations than the equivalent 2-D plate FEM models. [4,5,6] The comparison of our conventional 2-D FEM analysis and that of 3-D FEM analysis with experimental data shows that the eigenvalue analysis is more precise in 3-D FEM analysis. [7] A static condensed method and a half or a quarter model were also employed to further reduce calculation time and memory by as much as 40 times. [8] These improvements have made feasible the 3-D FEM analysis as a designing tool for commercial products. The calculated results of the frequency temperature curves were very precise and the prediction of frequency jumps by a spurious mode was relatively accurate when compared with experimental results.

The surface charge amount (hereafter it is defined as q) over the blank surface was also calculated. [9,10,11] We had proposed that the q by 2-D FEM analysis could be a good parameter for the evaluation of the coupling level with the spurious mode. [12] When there is a large change in q in main mode, there would be a strong coupling with other vibration mode and a big frequency shift caused by its coupling. In this paper, the numerical analysis of the q in various conditions of resonators were performed. It will be proposed that q is strongly related to the energy trapping of the main mode and furthermore the relative impedance. This correlation is verified by experimental measurements of their crystal impedances.

0-7803-7688-9/03/$17.00 © 2003 IEEE

II. FEM

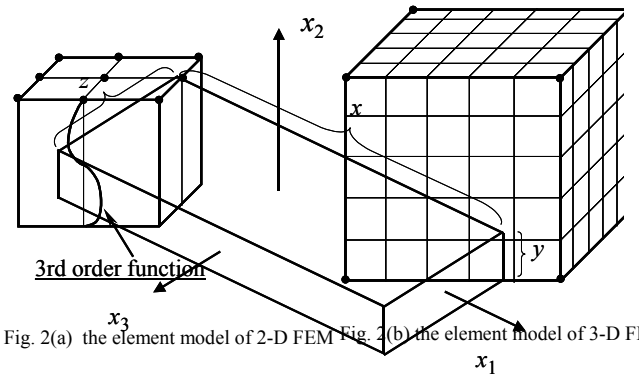

Fig. 2(a) the element model of 2-D FEM Fig. 2(b) the element model of 3-D FEM

Fig.1 the coordinates for a resonator

ANALY SIS

A. Element for 3-D FEM analysis

Fig 1 shows the coordinates of an AT-cut resonator.

The element model of a 2-D plate FEM and that of 3-D FEM used in this paper are shown in Fig. 2 (a) and Fig. 2 (b). Our conventional 2-D FEM analysis used a 9 nodes element with Mindlin's 3rd order equations. In the 3-D analysis, a single layer of 216-node(6x6x6) element was used. For example, the 13MHz resonator has the size ratio of 16x12. (The size ratio means the ratio of the length and width of the blank to the thickness.) In the 2-D plate FEM analysis, 100x70 elements (340,092 equations) were required to be solved. For the same resonator, the 3-D FEM model needed only 202,224 equations to provide more accurate results. We can further decrease the number of equations to about 156,264 by using 108-node (3x6x6) elements for the electrodes since the electrode films are very thin compared with the plate.

B. Static condensed method

In the piezoelectric problem, the electric potential degree of freedom is associated with the electrostatic problem. For quartz, the dielectric permittivities are more than 20 orders smaller than the elastic constants and the weak piezoelectric coupling constants are more than 10 orders smaller. Hence, when the electric degree of freedom is included in the finite element model, numerical problems arise from the weak condition of the stiffness matrix and the associated zero mass in the mass matrix. Sometimes this results in missing eigenvalues. In order to form a well-posed eigenvalue problem with positive definite mass matrix and a positive stiffness matrix, we statically condensed the electric potential degrees of freedom into the mechanical degree of freedom. As in eq.(1), we usually solve equations using the matrix with the coefficients related to both of mechanical and piezoelectric constants.

$$\begin{bmatrix} K_M & K_\varepsilon^T \\ K_\varepsilon & K_e \end{bmatrix} \begin{bmatrix} u \\ \phi \end{bmatrix} = \omega^2 \begin{bmatrix} M & 0 \\ 0 & 0 \end{bmatrix} \begin{bmatrix} u \\ \phi \end{bmatrix} \qquad \cdots (1)$$

Here u and ϕ represents the displacement and the electrical potential respectively. As in eq. (2), in a statically condensed method, the piezoelectric equations can be statically condensed into piezoelectrically stiffened mechanical equations.

By condensing our three electric degrees of freedom, the calculation time was improved by 20%. There were no missing eigenvalues or stacking of the calculation.

C. Mesh model

In our analyses, quarter models or half models were employed to reduce computation time and memory. The modes calculated in quarter models agreed with major spurious modes observed experimentally. The 216-node isoparametric element with quintic Lagrangean polynomial shape functions was used. The analysis of convex type resonator was also carried out using

$$\phi = -K_e^{-1} K_\varepsilon u,$$
$$(K_M - K_\varepsilon^T K_e^{-1} K_\varepsilon) u = \omega^2 M u \qquad \cdots (2)$$

quarter model. The results were sufficiently accurate for practical resonator design work. In this paper, most of FEM analyses were carried out by using quarter model.

A Compaq Alpha ES45 computer (CPU speed 1.25GHz, Memory 32GB 4cpus) was used for the FEM computations. Parallel computing is also employed in our analyses. For pre- and post-processing, a desktop PC was used.

III. ANALYTICAL/ EXPERIMENTAL RESULTS

A. Comparison between 2-D and 3-D FEM

Fig.3 (a) and Fig. 3 (b) show the frequency spectrum of 13MHz AT-cut quartz blanks calculated by 2-D Mindlin Plate FEM and our new 3-D FEM respectively. As explained in the previous paragraph, size ratios of the blank were 16 in *x* and 12 in *z* respectively. The quarter models were employed, and there were 85,000 degrees of freedom in 2-D Mindlin Plate FEM model and 30,000 degrees of freedom in the 3-D FEM model. The experimental results were also shown in both figures. Each spectrum was measured by a network analyzer by applying the electrical field on whole blank area through the air gap of 50 micro meter. The size of bubbles shows the vibration strength of each vibration mode. Although there was more than two times less number of equations in 3-D FEM model, it provided analytical results in good agreement with experimental results.

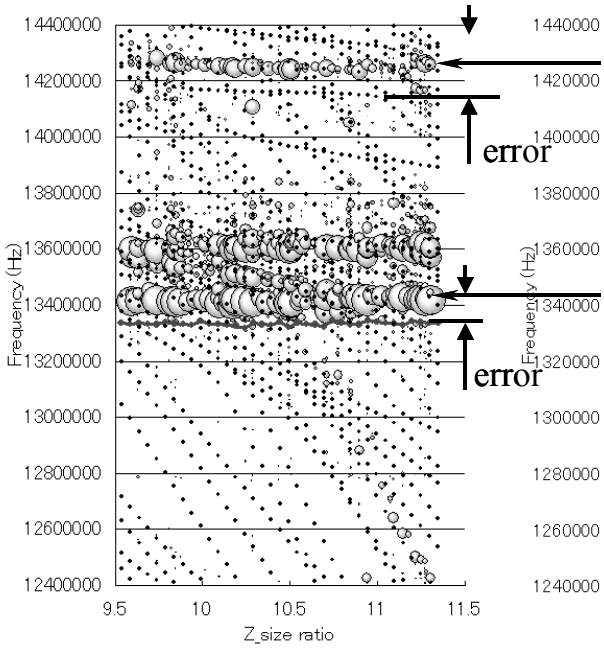

Fig. 3(a) the frequency spectrum by 2-D FEM Dots are calculated results and bubbles are experimental results.

The 2-D Mindlin Plate FEM model results however had larger errors, especially in the thickness shear modes. We thought this was perhaps due to the neglecting of piezoelectric effects in the model which accounts for the lower frequencies compared with the experimental data. However when the 3-D FEM results with no piezoelectric effect were obtained and compared with the 2-D Plate FEM results, we observed that the lower frequencies of the 2-D Plate FEM model were caused not only by the lack of piezoelectric effect but also by the approximation of the thickness shear mode by the third order polynomial thickness function of Mindlin's 3rd order plate theory. The 216-node 3-D element is more accurate because the displacement mode shape of the measured thickness shear mode is better described by its quintic polynomial shape functions.

B. Plated quartz crystal

Fig. 4 shows the frequency spectrum of the plated blanks. The silver electrodes with a thickness of 350 nm were deposited on both surfaces. 3-D FEM model takes into account the electrode material constants such as those of gold, silver and aluminum. We also confirmed that the predicted eigenvalues were in good agreement with the experimental data of plated resonators as well. Here the bubble size shows the admittance of each vibration mode. Careful comparison shows that major spurious modes with high admittance were calculated by the quarter FEM model. If one calculates a FEM model using the full model, one will notice that are additional vibration modes that do not exist in a practical resonator. These additional modes may be extremely weak and may be difficult to detect due to charge cancellations over the electrodes.

Fig.
Dot
exp

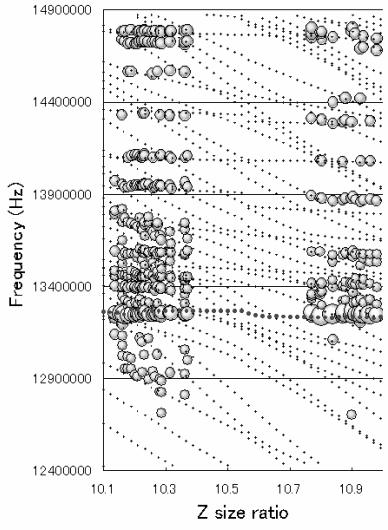

Fig.4 the frequency spectrum of the plated blanks

Frequency temperature curve was calculated for a plated resonator with *x* and *z* size ratio of 16.0 and 11.0 respectively. The calculated results were compared with experimental data. In Fig. 5, frequency responses at various temperatures were shown in the same figure as the change in frequency and in admittance at various temperatures. At 55°C, the thickness share mode was coupled with a neighboring spurious mode and lowered its admittance. In Fig. 6, the frequency temperature curve for all of measured vibration modes were shown. Thermal coefficients of all vibration modes were in good agreement and their frequencies were calculated with small errors. In Fig. 7(a), the change in admittance of the thickness shear mode (TS1) and that in the spurious mode which was coupled with TS1 around 55°C

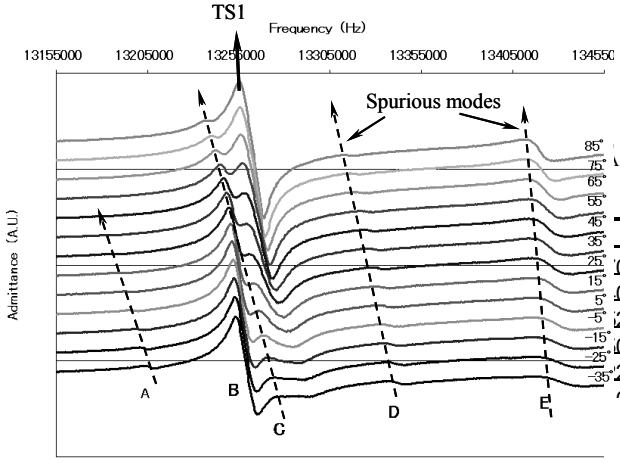

Fig.5 frequency responses at various temperatures

are shown. In Fig. 7(b), the change in calculated surface charge q of both vibration modes are also plotted. On mode coupling, change in q's of two vibration modes represented those changes in admittance very well.

C. Surface charge, q

In frequency-temperature curves, the calculated q embodied the change in admittance of practical resonator. The results of analyses in the previous sections demonstrate that the 3-D FEM model of BAW resonators yields frequencies (eigenvalues), which compare very well with the measured data. It follows that since the eigenvalues are accurately predicted, the eigenvectors should be accurate too. The eigenvectors are used for displaying mode shapes and for useful post-processing calculations of stresses and surface charges. The eigenvectors are not unique in that they can be scaled by a constant, just as the electric potential can be scaled by a constant factor in electrostatic problems. We propose that the coupling level with other spurious mode could be predicted by the calculation of a continuous change in surface charge obtained by our 3-D FEM analysis. [12] We further propose that surface charge q can be related to the reactive impedance and the energy trapping condition. Therefore, the post-processing calculation of these parameters would be also useful for predicting the crystal impedance of resonators under development.

For example, if surface charge q is related to the crystal impedance, the impedance determined by q (Zq) is expressed by following equation.

In general, the resonator impedance is determined by several factors. They are inertial loss caused by (1) crystal viscosity, (2) mechanical loss caused by the friction at the interface between crystal and electrode films, (3) electrical resistance along electrode lead and pad, (4) the mechanical loss at the supporting area, (5) the mechanical loss at the blank edge caused by the friction between crystal and atmosphere which is strongly related to the level of the energy trap of a blank, and (6) the mode coupling with spurious modes. In our FEM analysis, mechanical losses caused by friction or the inertial loss caused

$$Z_q = \frac{|V|}{|I|} = \frac{|V|}{\omega_0 \cdot q} \qquad \cdots (3)$$

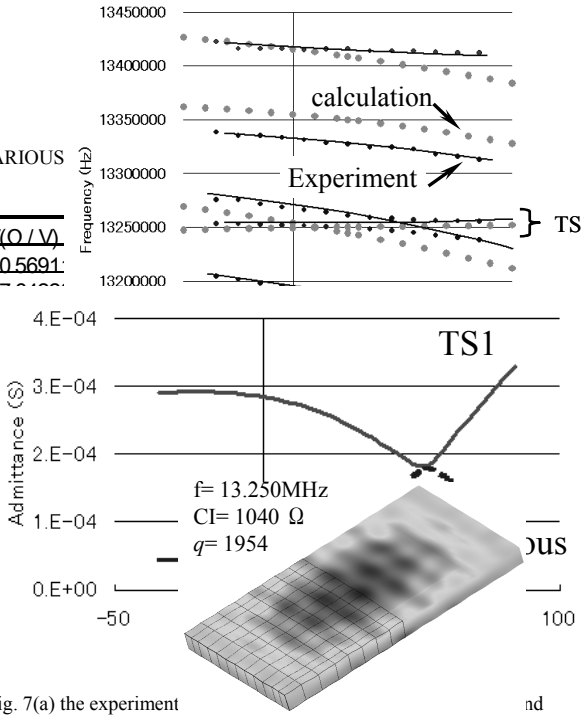

Fig. 7(a) the experiment and spurious mode

Fig. 8(a) the mode shape of TS1 of 13MHz plated resonator.(quarter model)

by a material viscosity was

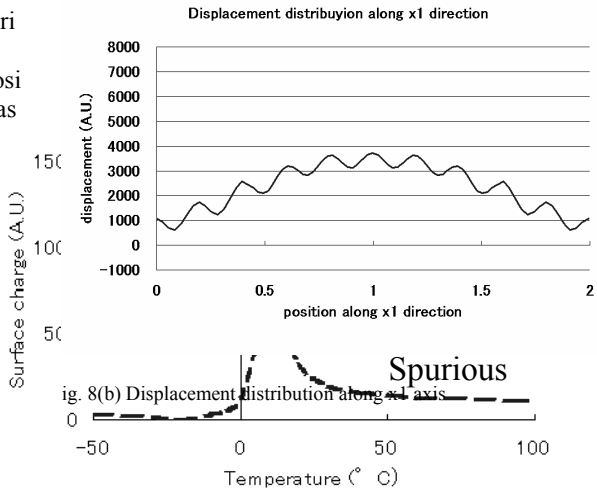

Fig. 8(b) Displacement distribution along x1 axis

Fig. 7(b) the calculated results – change in the q of TS1 and spurious mode

not modeled. So the term Zq of Eq. (3) takes into account only part of the actual impedance of the resonator. From our experimental results, the first three factors seemed to be very small in resonators with optimized designs. The minimum crystal impedance in a well-designed resonator is around 10 ohm. It is supposed that minimum impedance was determined mainly by first three factors. However, there are much higher impedances observed in many cases, such as in a coupling phenomenon with a spurious mode. In this condition, Zq would have strong relationship with their actual resonator impedances.

D. Surface charge amount q vs. resonator impedance

The q of various types of resonators were calculated and compared with their resonator impedances. In Table 1, the

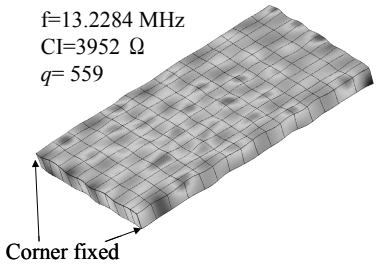

Fig. 9(a) the mode shape of TS1 of 13MHz plated resonator.(quarter model)

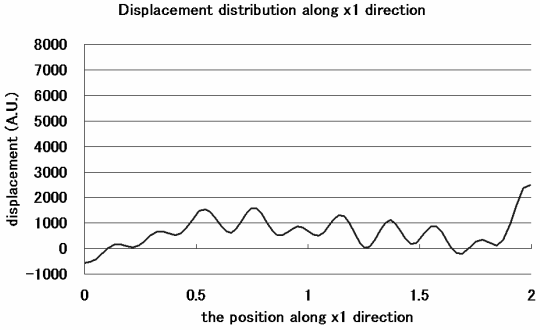

Fig. 9(b) Displacement distribution along x1 axis

resonator impedances and calculated *q* values of various type of resonators are shown along with the experimental data of commercial resonators at different frequencies.

The calculated mode shape has very useful information on the energy trapping condition of the resonator. In Figs. 8(a)-(b), the mode shape and the displacement distribution of the thickness shear mode (TS1) of a 13MHz plated quartz crystal blank are shown. This mode shape shows that the energy trapping of this resonator is not enough and that the mechanical vibration penetrates to the blank edge. Measured impedance was about 1K ohm. The resonator impedance was measured by an air gap type fixture, so that there are no supporting structures to affect to the experimental result. The *q* was calculated over the whole surface in this case. Then the blank was mounted into the package by fixing just the corner of the blank by a silver paste. The resonator impedance was measured through the electrode pad, so the *q* was calculated over the electrode area. The calculated result is shown in Figs.9 (a)-(b). The TS1 mode was severely suppressed by the supporting structure. The resonator impedance was 4K ohm. It was clear that the poor energy trapping caused a large increase in the resonator impedance and that the mechanical loss at the supporting structure is more critical than the mechanical loss by friction with the atmosphere at the blank edges in AT cut resonators.

The Eq. (3) can be rewritten as:

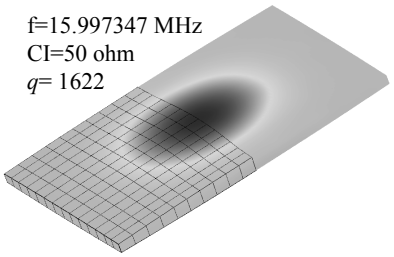

Fig. 10(a) the mode shape of TS1 of commercial 16MHz convex type resonator (quarter model)

The calculated $1/(\omega_0 \cdot q)$ is also shown in Table 1. As stated above, there are many factors determining resonator impedance. Fig 10 (a) shows the mode shape of a commercial 16MHz convex type resonator with *x* size ratio of 19 and with *z* size ratio of 13. The cross sectional view of the convex type blank is shown in Fig. 10 (b). From the displacement profile in Fig. 10 (c), the energy trapping was sufficient. This resonator was well designed and its crystal impedance was 50 ohm. Since a well-designed resonator like this is assumed to have the smallest mechanical losses by friction, we picked up a few well-designed resonators and compared their experimental results. In Fig. 11, the calculated $1/(\omega_0 \cdot q)$s were plotted with measured CI/V. (CI is the resonator impedance.) The calculated terms $1/(\omega_0 \cdot q)$'s were exactly proportional to the measured CI/V. Hence, if there are small effects of friction and inertial losses in a resonator, the resonator impedance can be estimated by the $1/(\omega_0 \cdot q)$ term calculated from the surface charge *q*.

IV. CONCLUSIONS

3-D FEM analysis was employed for the analysis of AT cut resonators. By using 216 nodes element, the computational time and memory were reduced when compared with the 2-D Mindlin Plate FEM. The static condensation of the electric potential degrees of freedom reduces the calculation time by 20%. Our calculated frequency spectrums were in good agreement with the experimental results for quartz crystal blank and plated blanks. The frequency temperature curves were also calculated precisely. This analytical method is useful for the designing work of commercial resonators. We proposed that the surface charge amount *q* is related to the reactive crystal impedance. It will be useful to use the $1/(\omega_0 \cdot q)$ value for estimation of unknown properties of new type of resonators.

$$\frac{Z_q}{|V|} = \frac{1}{\omega_0 \cdot q} \qquad \cdots (4)$$

ACKNOWLEDGEMENT

The authors deeply appreciate to Mr. Wu for his excellent work to make out the program code. Also we would like to thank to Mr. Endo, Mr. Unno and Mr. Ogura for their excellent work in fabricating the various shaped resonators; and to Mr. Zhang for his valuable advise and encouragement.

REFERENCES

1. "Accuracy of Crystal Plate Theories for High Frequency Vibrations in the Range of the Fundamental Thickness Shear Mode," Y-K Yong, Z. Zhang, and J. Hou, IEEE Transactions on Ultrasonics, Ferroelectrics, and Frequency Control, Vol. 43, No.5, Sept. 1996, pp888-892.

Fig. 10(b) Cross sectional view of the convex type blank

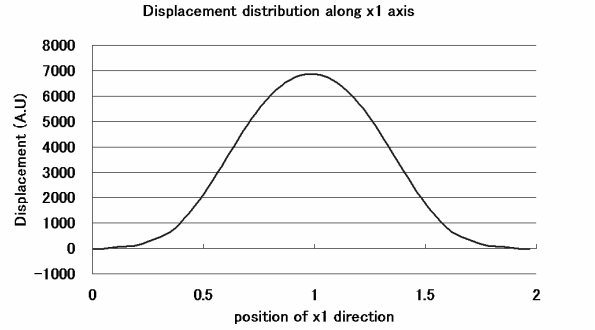

Fig. 10(c) Displacement distribution along x1 axis

2. "On the Accuracy of Mindlin Plate Predictions for the Frequency-Temperature Behavior of Resonant Modes in AT- and SC-cut Quartz Plates", Y-K Yong, J. Wang and T. Imai, IEEE Transactions on Ultrasonics, Ferroelectrics, and Frequency Control, Vol. 46, No. 1, January 1999, pp 1-14.

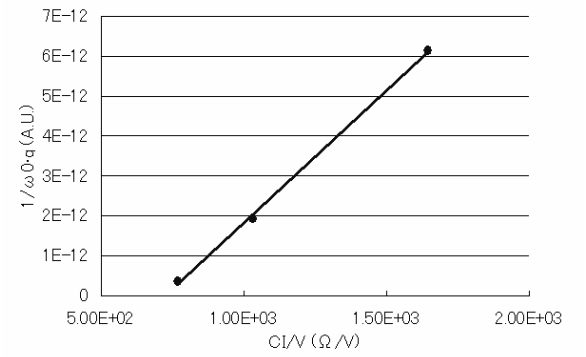

Fig.11 the calculated $1/\omega_0 \cdot q$ vs. Measured CI/V

3. "Finite Element Analysis of the Piezoelectric Vibrations of Quartz Plate Resonators with Higher Order Plate Theory", J. Wang, Y-K Yong and T. Imai, International Journal of Solids and Structures, Vol. 36, 1999, pp 2303-2319.
4. "Frequency-temperature Behavior of Thickness Vibrations of Doubly Rotated Quartz Plates affected by Plate Dimensions and Orientations," P.C.Lee and Y-K. Yong, J. of Appl. Phys., 60, pp2327-2342.
5. "Theoretical Analysis of Quartz Resonators and Finite Element Applications," Y-K. Yong, Proc. Of 27th EM Symposium, 1998,pp51-65.
6. "Higher Order Plate Theory Based Finite Element Analysis of the Frequency-temperature Relations of Quartz Crystal Resonators," J. Wang, Y-K.Yong, and T.Imai, Proc. of Freq. Cont. Symp. 1998, pp956-963.
7. "Three dimensional finite elements and their relationships to Mindlin's higher order plate theory in Quartz crystal plate", Y-K. Yong, W. Wei, M. Tanaka and T.Imai, Proc. of Freq. Cont. Symp. 2001, pp791-794.
8. "Finite Element Method for Piezoelectric Vibration", H. Allik and T.J.R. Hughes, *International Journal for Numerical Methods in Engineering*, Vol. 2, 1970, pp. 151-157.
9. "Forced Vibrations of Thickness-flexures, Face-shear and Face-flexure in rectangular AT-cut Quartz Plates," Proc. IEEE Freq. Cont. Symp., 1992, pp 532-536.
10. "Three Dimensional Analysis of Forced Vibrations of Rectangular AT-cut Quartz Plates," A.Ishizaki and H.Sekimoto, IEEE Freq. Cont. Symp., 1998, pp942-946.
11. "Linear Piezoelectric Plate Vibrations", H.F.Tiersten, Plenum, 1969, pp185-187.
12. "Surface charge measurement/calculations for the prediction of spurious modes and frequency jumps in AT-cut quartz resonators", T. Imai, M. Tanaka, Y-K. Yong, Proc. of Freq. Cont. Symp. 2001, pp 616-622.